DMD Fast Forward. Published on February 15, 2017 as DOI: 10.1124/dmd.116.074104
This article has not been copyedited and formatted. The final version may differ from this version.

DMD # 74104

Nimesulide and 4'-Hydroxynimesulide as Bile Acid Transporters Inhibitors are Contributory Factors for Drug-Induced Cholestasis

Lei Zhou, Xiaoyan Pang, Jingfang Jiang, Dafang Zhong, and Xiaoyan Chen

Shanghai Institute of Materia Medica, Chinese Academy of Sciences, Shanghai 201203, China (L.Z., X.P., J.J., D.Z., X.C.)

University of Chinese Academy of Sciences, Beijing 100049, China (L.Z., J.J., D.Z., X.C.)

Downloaded from dmd.aspetjournals.org at ASPET Journals on April 18, 2024

DMD Fast Forward. Published on February 15, 2017 as DOI: 10.1124/dmd.116.074104
This article has not been copyedited and formatted. The final version may differ from this version.

Running Title

Nimesulide and Its Metabolite Inhibit Bile Acid Transporters

Corresponding Author

Xiaoyan Chen

Shanghai Institute of Materia Medica, Chinese Academy of Sciences, 501 Haike Road, Shanghai 201203, China

Tel/Fax: +86-21-50800738

E-mail: xychen@simm.ac.cn

Pages: 18

Tables: 3

Figures: 9

References: 38

Abstracts: 219 words

Introduction: 465 words

Discussion: 1166 words

Abbreviations: ALP, alkaline phosphatase; ALT, alanine aminotransferase; AST, aspartate aminotransferase; AUC, area under the plasma concentration-time curve; BEI, biliary excretion index; BSEP, bile salt export pump; CA, Cholic acid; CDCA, chenodeoxycholic acid; CDF, 5 (and 6)-carboxy-2',7'-dichlorofluorescein; CDFDA, 5 (and 6)-carboxy-2',7'-dichlorofluorescein diacetate; $Cl_{biliary}$, biliary clearance; CMC-Na, sodium carboxymethyl cellulose; CyA, cyclosporine A; DCA, deoxycholic acid; FBS, fetal bovine serum; GCA, glycocholic acid; GCDCA,

Downloaded from dmd.aspetjournals.org at ASPET Journals on April 18, 2024

DMD Fast Forward. Published on February 15, 2017 as DOI: 10.1124/dmd.116.074104
This article has not been copyedited and formatted. The final version may differ from this version.

glycochenodeoxycholic acid; GDCA, glycodeoxy cholic acid; GUDCA, glycoursodeoxycholic acid; HBSS, Hank's balanced salt solution; LCA, lithocholic acid; LC-MS/MS, liquid chromatography-tandem mass spectrometry; M1, 4'-hydroxynimesulide; M2, nitro-reduced NIM; M4, acetylated metabolite of M2; MRM, multiple reaction monitoring; MRP, multidrug resistance-associated protein; NIM, nimesulide; NTCP, Na^+-taurocholate contransporting polypeptide; OATP, organic anion transporting protein; TBA, total bile acid; TCA, taurocholic acid; TCDCA, taurochenodeoxycholic acid; UDCA, ursodeoxycholic acid.

Downloaded from dmd.aspetjournals.org at ASPET Journals on April 18, 2024

DMD Fast Forward. Published on February 15, 2017 as DOI: 10.1124/dmd.116.074104
This article has not been copyedited and formatted. The final version may differ from this version.

Abstract

Nimesulide (NIM) is a classic nonsteroidal anti-inflammatory drug. However, some patients treated with NIM suffered from cholestatic liver injury. For this reason, we investigated the potential mechanism underlying NIM-induced cholestasis by using in vivo and in vitro models. Oral administration of 100 mg/kg/day NIM to Wistar rats for 5 days increased the levels of plasma total bile acids, alkaline phosphatase, alanine aminotransferase, and aspartate aminotransferase by 1.49-, 1.31-, 1.60-, and 1.29-fold, respectively. In sandwich-cultured rat hepatocytes, NIM and 4′-hydroxynimesulide (M1) reduced the biliary excretion index of d_8-taurocholic acid (d_8-TCA) and 5 (and 6)-carboxy-2′,7′-dichlorofluorescein in a concentration-dependent manner, indicating the inhibition of the efflux transporters bile salt export pump and multidrug resistance-associated protein 2, respectively. In suspended rat hepatocytes, NIM and M1 inhibited the uptake transporters of d_8-TCA for Na^+-taurocholate cotransporting polypeptide at IC_{50} values of 21.3 and 25.0 μM, respectively, and for organic anion transporting proteins at IC_{50} values of 45.6 and 39.4 μM, respectively. By contrast, nitro-reduced NIM and the further acetylated metabolite did not inhibit or they only marginally inhibited these transporters at the maximum soluble concentrations. Inhibitory effects of NIM and M1 on human bile acid transporters were also confirmed using sandwich-cultured human hepatocytes. These data suggest that inhibition of bile acid transporters by NIM and M1 is one of the biological mechanisms of NIM-induced cholestasis.

Downloaded from dmd.aspetjournals.org at ASPET Journals on April 18, 2024

DMD Fast Forward. Published on February 15, 2017 as DOI: 10.1124/dmd.116.074104
This article has not been copyedited and formatted. The final version may differ from this version.

Introduction

Nimesulide (NIM) is a classic nonsteroidal anti-inflammatory drug that selectively inhibits cyclooxygenase-2. It has been marketed in more than 50 countries since 1985. However, severe liver injury has been reported in some patients who received NIM treatment. Thus, the use of NIM was restricted, and NIM was even withdrawn from the market in some countries. Clinically, NIM-induced liver injury is mainly characterized by two patterns: hepatocellular necrosis and cholestasis (Romero-Gomezz et al., 1999; Stadlmann et al., 2002). Metabolic activation may be associated with the hepatotoxicity of NIM (Li et al., 2008). Studies by our group has demonstrated that oxidative and reductive activation of NIM do not cause the toxicity in primary human and rat hepatocytes (Zhou et al., 2015). The mitochondrial toxicity of the parent drug may play a critical role in NIM-induced rat hepatocellular toxicity (Mingatto et al., 2002). Until now, the mechanism of NIM-induced cholestasis remains unclear.

Inhibition of bile acid transporters has been implicated in drug-induced cholestasis (Stieger et al., 2000; Kostrubsky et al., 2003; Dawson et al., 2012; Li et al., 2015; Slizgi et al., 2016). The major transport proteins responsible for the basolateral uptake of bile acids are Na^+-taurocholate cotransporting polypeptide (NTCP) and organic anion transporting proteins (OATPs). After entering the hepatocytes, bile acids are mainly excreted into canaliculus via the bile salt export pump (BSEP) and multidrug resistance-associated protein 2 (MRP2) on the canalicular membrane (Alrefai and Gill, 2007; Halilbasic et al., 2013). A previous study (Saab et al., 2013)

Downloaded from dmd.aspetjournals.org at ASPET Journals on April 18, 2024

DMD Fast Forward. Published on February 15, 2017 as DOI: 10.1124/dmd.116.074104
This article has not been copyedited and formatted. The final version may differ from this version.

demonstrated that 450 μM of NIM inhibited the efflux of 5 (and 6)-carboxy-2′,7′-dichlorofluorescein (CDF) in HepG2 cells; therefore, NIM was concluded to inhibit MRP2. However, this conclusion is apparently insufficiently rigorous. CDF is a substrate for both MRP2 and basolateral efflux transporter MRP3 (Chandra et al., 2005), and reduced CDF efflux is possibly caused by inhibition of MRP2 or MRP3 or both. Moreover, the effects of NIM on other bile acid transporters remain unknown.

NIM undergoes extensive metabolism in humans (Gandini et al., 1991; Carini et al., 1998; Macpherson et al, 2013). The principal metabolic pathways include phenoxy ring hydroxylation to generate 4′-hydroxynimesulide (M1), reduction of the nitro group (M2) and subsequent acetylation (M4) (Fig. 1). M1 is the major circulating metabolite, and its AUC (area under the plasma concentration-time curve) is about 67% that of the parent drug. NIM is excreted by the renal route, mainly as M1 and its glucuronide (~18%), M2, M4, and their derivative (~20%). The effects of these metabolites on bile acid transporters also remain unclear.

In the present study, the cholestatic effect of NIM in rats was elucidated, and the effects of NIM and its main metabolites on bile acid transporters were studied using sandwich-cultured human and rat hepatocytes and isolated suspended rat hepatocytes. Our results revealed a potential mechanism of NIM-induced cholestasis.

Materials and Methods

Chemicals and Reagents

Downloaded from dmd.aspetjournals.org at ASPET Journals on April 18, 2024

DMD Fast Forward. Published on February 15, 2017 as DOI: 10.1124/dmd.116.074104
This article has not been copyedited and formatted. The final version may differ from this version.

All reagents used in cell culture were supplied by Invitrogen (Carlsbad, CA, USA) unless otherwise stated. D_5-taurocholic acid (d_5-TCA) and d_8-taurocholic acid (d_8-TCA) were purchased from Martrex, Inc. (Minnetonka, MN, USA). Cholic acid (CA), deoxycholic acid (DCA), chenodeoxycholic acid (CDCA), ursodeoxycholic acid (UDCA), lithocholic acid (LCA), glycocholic acid (GCA), glycodeoxycholic acid (GDCA), glycochenodeoxycholic acid (GCDCA), glycoursodeoxycholic acid (GUDCA), taurochenodeoxycholic acid (TCDCA), and TCA were purchased from Toronto Research Chemicals, Inc. (North York, ON, Canada). M1, M2 and M4 were synthesized according to reported methods (Küçükgüzel SG et al., 2005; Li et al., 2008); MS and ^{1}H NMR analyses were applied to confirm these metabolites, which were >98% pure. The assay kits for total bile acid (TBA), alkaline phosphatase (ALP), alanine aminotransferase (ALT) and aspartate aminotransferase (AST) were purchased from Nanjing Jiancheng Bioengineering Institute (Jiangsu, China). Bicinchoninic acid (BCA) protein assay kit was purchased from Beyotime (Jiangsu, China). All other solvents and reagents were obtained from Sigma-Aldrich (St. Louis, MO, USA).

Animal Experiments

All procedures in animal studies were performed in accordance with the *Guide for the Care and Use of Laboratory Animals* of Shanghai Institute of Materia Medica, Chinese Academy of Sciences. Male Wistar rats weighing 200–250 g were randomized into two groups (n = 6/group). One group of rats were orally administrated with 100 mg/kg/day NIM formulated in 0.5% sodium carboxymethyl

Downloaded from dmd.aspetjournals.org at ASPET Journals on April 18, 2024

DMD Fast Forward. Published on February 15, 2017 as DOI: 10.1124/dmd.116.074104
This article has not been copyedited and formatted. The final version may differ from this version.

cellulose (CMC-Na) for 5 successive days, and the other group of rats were orally administrated with the corresponding vehicle control. At 24 h after the last dose, the animals were anesthetized and sacrificed through exsanguination. Their livers were collected and frozen at −80 °C. Plasma samples were obtained by centrifugation of blood samples at 11,000 rpm for 5 min and then frozen at −80 ℃ until further analysis. Plasma ALP, ALT and AST levels were determined using the corresponding assay kits according to the manufacturer's protocol. For the bile flow studies, two groups of rats (n = 4/group) were treated with the same dosage regimen mentioned above. At 24 h after the last dose, the animals were anesthetized and placed on their backs under a heat lamp to maintain their body temperature at 37 ℃. The bile duct was subsequently cannulated with a polyethylene tube. After an equilibration period of 30 min, bile was collected every 30 min for 2.5 h. After the last sample collection, the rats were sacrificed and their livers were collected. The TBA levels in rat plasma and bile were determined using TBA assay kit according to the manufacturer's protocol. The concentrations of 11 bile acids in rat plasma and liver were determined using liquid chromatography-tandem mass spectrometry (LC-MS/MS) as described by Li et al (2015).

Hepatocytes Isolation and Culture

Rat hepatocytes were isolated from male Wistar rats using a collagenase perfusion as previously described (Zhou et al., 2015). Fresh rat hepatocytes were seeded at a density of 6.0 $\times 10^5$ cells/ml in a 48-well plates precoated with rat tail collagen and then cultured in Williams'E medium supplemented with 0.1 μM

Downloaded from dmd.aspetjournals.org at ASPET Journals on April 18, 2024

DMD Fast Forward. Published on February 15, 2017 as DOI: 10.1124/dmd.116.074104
This article has not been copyedited and formatted. The final version may differ from this version.

dexamathasone, 5% fetal bovine serum (FBS), 100 U penicillin, 100 μg/ml streptomycin, 2 mM glutamine, and 1% ITS. After incubation for 4 h at 37 ℃ in a humidified incubator containing 95% O_2/5%CO_2, a serum-free Williams'E medium containing 0.1 μM dexamathasone, 100 U penicillin, 100 μg/ml streptomycin, 2 mM glutamine, and 1% ITS was used to replace the plating medium, and the hepatocytes were overlaid with 0.25 mg/ml of ice-cold Matrigel to form a sandwich configuration (McRae et al., 2006; Li et al., 2015). The serum-free Williams'E medium was replaced every 24 hours until the experiments were conducted. Rat hepatocytes cultured for 4 h could be directly used for the transporter-mediated uptake assays.

Cryopreserved primary human hepatocytes (lot no. 393A: Caucasian female; aged 29) were obtained from BD Gentest (Woburn, MA, USA) and were treated in a similar fashion to rat hepatocytes except that human hepatocytes were seeded at a density of 7.0 ×10^5 cells/ml in a 24-well plates precoated with rat tail collagen.

Accumulation Studies in Sandwich-cultured Hepatocytes

Accumulation studies were conducted on day 4 of culture for rat hepatocytes and day 5 for human hepatocytes. Hepatocytes were rinsed three times with either standard HBSS or Ca^{2+}-free HBSS and then equilibrated with the same buffer in the presence of test compounds (0–400 μM NIM or M1, 0–400 μM M2, 0–200 μM M4, 10 μM cyclosporine A (CyA), and 20 μM MK-571) for 10 min at 37 ℃. The highest concentrations were set as the limit of solubility for each analyte. Incubation in standard HBSS maintains the integrity of tight junctions, whereas incubation in Ca^{2+}-free HBSS disrupts tight junctions, leading to the release of bile acid from

Downloaded from dmd.aspetjournals.org at ASPET Journals on April 18, 2024

DMD Fast Forward. Published on February 15, 2017 as DOI: 10.1124/dmd.116.074104
This article has not been copyedited and formatted. The final version may differ from this version.

canaliculi. After the initial incubation, the hepatocytes were incubated with standard HBSS containing probe substrates (1 μM d_8-TCA and 2 μM 5 (and 6)-carboxy-2′,7′-dichlorofluorescein diacetate (CDFDA)) and test compounds for another 10 min. Subsequently, the transport was quenched by removing the buffer and rinsing the cells three times with ice-cold standard HBSS. CDF accumulation in bile canaliculi was visualized using a fluorescence microscope (Olympus, Tokyo, Japan). The hepatocytes were subsequently lysed with 200 μl of 0.1% Triton X-100 (v/v) in deionized water and then vortexed gently for 30 min at room temperature prior to CDF analysis at 488 nm (excitation) and 525 nm (emission) by using a microplate fluorescence reader (Molecular Devices, Sunnyvale, CA, USA). The hepatocytes treated with d_8-TCA were lysed with 200 μl of deionized water followed by three freeze-thaw cycles and then stored at −80 °C until LC-MS/MS analysis. The amount of substrates accumulated in each well was corrected with protein concentration as measured by a BCA protein assay kit.

Efflux Studies in Sandwich-cultured Hepatocytes

According to previously reported methods (Guo et al., 2014), the rat hepatocytes were pre-incubated with standard HBSS for 10 min at 37 ℃ and then incubated with 2 μM CDFDA or 1 μM d_8-TCA in standard HBSS for another 10 min. At the end of incubation, the hepatocytes were quickly washed with ice-cold standard HBSS three times to terminate the accumulation process. The efflux was initiated by incubating the cells with warm standard HBSS containing inhibitors (0–200 μM NIM or M1 and 20 μM MK-571). After 20 min of incubation at 37 ℃, the efflux medium was

Downloaded from dmd.aspetjournals.org at ASPET Journals on April 18, 2024

DMD Fast Forward. Published on February 15, 2017 as DOI: 10.1124/dmd.116.074104
This article has not been copyedited and formatted. The final version may differ from this version.

collected for analysis.

d_8-TCA Uptake Inhibition Assay

To investigate the effects of NIM and its metabolites on NTCP- and OATP-mediated uptake of d_8-TCA by rat hepatocytes, the Na^+ in standard HBSS was replaced with choline chloride. The hepatocytes were rinsed three times with standard HBSS or with choline chloride buffer and then pretreated in the same buffer with test compounds (0–400 μM NIM or M1, 0–400 μM M2, 0–200 μM M4, and 10 μM CyA) for 10 min. The uptake assay was initiated by adding standard HBSS containing 1 μM d_8-TCA and test compounds. After 2 min of incubation, the cells were quickly rinsed three times with ice-cold standard HBSS and then lysed by adding 200 μl of deionized water.

Sample Pretreatment

To measure NIM and related metabolites in rat plasma, 25 μl of sample was mixed with 25 μl of internal standard (10 μg/ml glycyrrhetinic acid for determination of NIM, M1 and M4; and 20 ng/ml propafenone for determination of M2) and 100 μl of acetonitrile. After vortexing and centrifugation at 11,000 g for 5 min, the supernatant was injected into the LC-MS/MS system for analysis. The rat livers (200 mg) were homogenized in 1 ml of ethanol/water (1:1, v/v) followed by ultrasonication for 20 min. The resulting liver homogenate was treated in a manner similar to that described for plasma.

For the samples obtained from transporter assays, 50 μl of sample was added into a mixture containing 25 μl of internal standard (20.0 ng/ml d_5-TCA) and 100 μl of

Downloaded from dmd.aspetjournals.org at ASPET Journals on April 18, 2024

DMD Fast Forward. Published on February 15, 2017 as DOI: 10.1124/dmd.116.074104
This article has not been copyedited and formatted. The final version may differ from this version.

acetonitrile followed by vortexing and centrifugation. The resultant supernatant was analyzed by LC-MS/MS.

LC-MS/MS Analysis

The LC system consisted of a LC-30AD pump equipped with a SIL-30AC autosampler (Shimadzu, Kyoto, Japan). An Eclipse Plus C18 (100 × 2.1 mm i.d., 3.5 μm; Agilent) column was used to simultaneously determine NIM, M1, and M4. The mobile phase consisted of 5 mM ammonium acetate and acetonitrile (40:60, v/v) at a flow rate of 0.5 ml/min. An Eclipse Plus C18 (100 × 4.6 mm i.d., 3.5 μm; Agilent) column was used to analyze M2. The mobile phase consisted of a mixture of 5 mM ammonium acetate containing 0.1% formic acid and acetonitrile (40:60, v/v) at a flow rate of 0.6 ml/min. d_8-TCA was quantitatively determined according to the method described by Li et al (2015).

MS detection was performed using an AB Sciex Triple Quad 5500 System (Applied Biosystems, Concord, ON, Canada) equipped with a TurboIonSpray ion source. Multiple reaction monitoring was used to quantify compounds in the positive ion mode (*m/z* 279.0 → *m/z* 200.0 for M2; and *m/z* 341.7 → *m/z* 115.9 for the internal standard propafenone) or in the negative ion mode (*m/z* 307.0 → *m/z* 229.0 for NIM; *m/z* 323.1 → *m/z* 245.1 for M1; *m/z* 319.1 → *m/z* 239.1 for M4; and *m/z* 469.2 → *m/z* 425.3 for the internal standard glycyrrhetinic acid).

Data Analysis

All mass values were normalized to the protein content (milligrams of protein per well). The accumulation in standard HBSS represents the total mass of uptaken

Downloaded from dmd.aspetjournals.org at ASPET Journals on April 18, 2024

DMD Fast Forward. Published on February 15, 2017 as DOI: 10.1124/dmd.116.074104
This article has not been copyedited and formatted. The final version may differ from this version.

and excreted compound (cell plus bile), whereas the accumulation in Ca^{2+}-free HBSS represents the mass of compound in the hepatocyte (cell only). Biliary excretion index (BEI), in vitro biliary clearance ($Cl_{biliary}$), and basolateral efflux were calculated according to the following equations (Liu et al., 1999; Guo et al., 2014).

$$\mathrm{BEI}(\%) = \frac{\mathrm{Accumulation}_{(\mathrm{Standard\ \ HBSS})} - \mathrm{Accumulation}_{(\mathrm{Ca^{2+}-free\ HBSS})}}{\mathrm{Accumulation}_{(\mathrm{Standard\ \ HBSS})}} \times 100 \quad (1)$$

$$\mathrm{Cl}_{\mathrm{biliary}} = \frac{\mathrm{Accumulation}_{(\mathrm{Standard\ \ HBSS})} - \mathrm{Accumulation}_{(\mathrm{Ca^{2+}-free\ HBSS})}}{\mathrm{time} \times \mathrm{concentration}_{\mathrm{medium}}} \quad (2)$$

$$\mathrm{Basolateral\ efflux} = \mathrm{total\ mass\ in\ efflux\ medium}_{\mathrm{Standard\ \ HBSS}} \quad (3)$$

For rat hepatocyte experiments, all data were compiled from at least three separate rat liver preparations and are presented as mean ± standard deviation (SD). Statistical analysis was performed using GradphPad Prism 5.0 software. Unpaired, two-tailed Student's *t*-test was used for between-group comparisons: $^{*}P < 0.05$, $^{**}P < 0.01$, and $^{***}P < 0.001$ indicated statistical significance.

Results

Cholestatic Effect of NIM in Rats

To assess the cholestatic effect of NIM, the AST, ALT, ALP, and TBA levels in rat plasma were measured. Relative to those in the control group, the plasma AST, ALT, ALP, and TBA levels in NIM-administered rats increased to 129%, 160%, 131%, and 149%, respectively (Figs. 2, A and B). The individual level of bile acid, including CA, DCA, CDCA, UDCA, LCA, GCA, GDCA, GCDCA, GUDCA, TCA,

Downloaded from dmd.aspetjournals.org at ASPET Journals on April 18, 2024

DMD Fast Forward. Published on February 15, 2017 as DOI: 10.1124/dmd.116.074104
This article has not been copyedited and formatted. The final version may differ from this version.

and TCDCA, in rat plasma and liver was measured by using a LC-MS/MS method. As shown in Table 1, the levels of unconjugated bile acid CA, DCA, CDCA, and UDCA in rat plasma significantly increased in NIM group compared with those in the control group (> 2-fold), but the levels of conjugated bile acids did not change. In rat liver, a significant elevation of CA, CDCA, and GCDCA levels was also observed (Table 2).

The biliary secretion of bile acids significantly decreased in the NIM group compared with that in the control group (Fig. 2C). However, no significant change was observed in the bile flow (Fig. 2D).

Metabolism of NIM in Rats

NIM and its three major metabolites (M1, M2, and M4) were detected in rat plasma and liver tissue at 24 h after the last dose. The concentrations of NIM, M1, M2, and M4 were quantified by using the LC-MS/MS method, and results are shown in Table 3.

Hepatobiliary Disposition of d_8-TCA in Sandwich-cultured Rat Hepatocytes

The hepatobiliary disposition of d_8-TCA is dependent on the uptake transporters NTCP and OATPs and on the efflux transporter BSEP (Lepist et al., 2014; Li et al., 2015; Slizgi et al., 2016). In sandwich-cultured rat hepatocytes, NIM and M1 reduced d_8-TCA cellular accumulation and cellular plus biliary accumulation in a concentration-dependent manner (Fig. 3A). The BEI and $Cl_{biliary}$ values of d_8-TCA in control group were 72.5% and 4.99 µl/min/mg protein, respectively (Fig. 3A). NIM (400 µM) reduced the BEI and $Cl_{biliary}$ values to 51.6% and 0.50 µl/min/mg protein,

Downloaded from dmd.aspetjournals.org at ASPET Journals on April 18, 2024

DMD Fast Forward. Published on February 15, 2017 as DOI: 10.1124/dmd.116.074104
This article has not been copyedited and formatted. The final version may differ from this version.

respectively; moreover, M1 (400 μM) reduced the BEI and $Cl_{biliary}$ values to 48.4% and 0.39 μl/min/mg protein, respectively. Similar results were observed for CyA, a potent inhibitor of NTCP, OATPs, and BSEP (Ansede et al., 2010; Li et al., 2015). In addition, a greater extent of reduction was found in $Cl_{biliary}$ than in BEI after NIM and M1 treatments (Fig. 3B). In M2 and M4 treatments, $Cl_{biliary}$ slightly decreased and BEI remained unchanged (Fig. 3B).

Inhibition of Uptake Transporters in Isolated Rat Hepatocytes

The suspended rat hepatocytes were used to examine the inhibitory effect of compounds on rat NTCP and OATPs. OATP-mediated d_8-TCA uptake is independent of Na^+, whereas the NTCP-mediated d_8-TCA uptake is dependent on Na^+ (Marion et al., 2011; Li et al., 2015). Thus, d_8-TCA uptake in cells incubated in choline chloride buffer (Na^+-free) is considered OATP-mediated uptake; NTCP-mediated uptake is defined as the difference in uptake by cells incubated in standard HBSS (Na^+-containing buffer) and choline chloride buffer (Na^+-free buffer). As shown in Fig. 4A, d_8-TCA uptake in the presence of Na^+ was approximately 4.2 times of that in the absence of Na^+, suggesting that NTCP was the major transporter mediating d_8-TCA uptake; this finding was consistent with that of earlier studies (Marion et al., 2011; Li et al., 2015). Similar to CyA, NIM and M1 greatly inhibited d_8-TCA uptake both in Na^+-containing and Na^+-free buffers. However, M2 and M4 did not inhibit d_8-TCA uptake in Na^+-containing buffer, and they exerted only weak inhibitory effects on d_8-TCA uptake in Na^+-free buffer. The inhibition potencies of NIM and M1 on rat NTCP and OATPs were characterized in terms of mean inhibitory

Downloaded from dmd.aspetjournals.org at ASPET Journals on April 18, 2024

DMD Fast Forward. Published on February 15, 2017 as DOI: 10.1124/dmd.116.074104
This article has not been copyedited and formatted. The final version may differ from this version.

concentration (IC_{50}). NIM inhibited NTCP- and OATP-mediated d_8-TCA uptake at IC_{50} values of 21.3 and 45.6 μM, respectively; by contrast, M1 inhibited NTCP- and OATP-mediated d_8-TCA uptake at IC_{50} values of 25.0 and 39.4 μM, respectively (Figs. 4, B and C).

Hepatobiliary Disposition of CDF in Sandwich-cultured Rat Hepatocytes

After its passive diffusion into hepatocytes, CDFDA is hydrolyzed into CDF by esterase. Subsequently, CDF, which is a fluorescent bile acid analog, is excreted either into bile by MRP2 or into blood by MRP3 (Zamek-Gliszczynski et al., 2003). On day 4 of culture, CDF accumulated within the canalicular network in sandwich-cultured rat hepatocytes as demonstrated by fluorescent microscopy (Fig. 5A). MK-571, a well-known MRP2 inhibitor, rendered the fluorescence in bile canaliculi undetectable (Fig. 5F). Similarly, 200 μM of NIM and M1 significantly reduced the fluorescent signal in the bile canaliculi (Figs. 5, B and C). Nevertheless, 400 μM of M2 and 200 μM of M4 did not inhibit or only slightly reduced the fluorescent signal in the bile canaliculi (Figs. 5, D and E).

Furthermore, CDF accumulation in cells incubated in the standard and Ca^{2+}-free buffers was quantified using a microplate fluorescence reader. NIM and M1 increased CDF cellular accumulation and cellular plus biliary accumulation in a concentration-dependent manner (Fig. 6). The BEI of CDF was 26.2% in control group, consistent with the reported BEI value of CDF in Wistar rat hepatocyte cultures (30%) (Zhang et al., 2005). A concentration-dependent reduction in BEI was observed both under NIM and M1 treatments. NIM and M1 (200 μM each) reduced

Downloaded from dmd.aspetjournals.org at ASPET Journals on April 18, 2024

DMD Fast Forward. Published on February 15, 2017 as DOI: 10.1124/dmd.116.074104
This article has not been copyedited and formatted. The final version may differ from this version.

the BEI of CDF to 13.0% and 5.3%, respectively. Nevertheless, no reduction or weak reduction in BEI was observed under M2 and M4 treatments.

Compared with that in the control group, the basolateral efflux of CDF under NIM and M1 treatments decreased in a concentration-dependent manner (Fig. 7). The basolateral efflux of CDF decreased to 49.9% and 38.9% of control following 20 min incubation with 200 μM NIM and M1, respectively.

Hepatobiliary Disposition of d_8-TCA and CDF in Sandwich-cultured Human Hepatocytes

In sandwich-cultured human hepatocytes, the cellular accumulation and cellular plus biliary accumulation of d_8-TCA decreased in a concentration-dependent manner under NIM and M1 treatments (Fig. 8). The BEI and $Cl_{biliary}$ values of d_8-TCA in control group were 78.5% and 17.2 μl/min/mg protein, respectively. NIM (400 μM) decreased the BEI and $Cl_{biliary}$ values to 65.0% and 3.73 μl/min/mg protein, respectively; moreover, M1 (400 μM) decreased the BEI and $Cl_{biliary}$ values to 71.8% and 7.12 μl/min/mg protein, respectively. In addition, 200 μM of NIM and M1 significantly decreased the fluorescent signal of CDF in the bile canaliculi, similar to the effect of MK-571 (Fig. 9).

Discussion

Cholestatic liver injury has been reported in some patients who received NIM treatment (Romero-Gomez et al., 1999; Stadlmann et al., 2002). In the present studies, we explored the cholestatic effect of NIM in rats, and further evaluated the effects of

Downloaded from dmd.aspetjournals.org at ASPET Journals on April 18, 2024

DMD Fast Forward. Published on February 15, 2017 as DOI: 10.1124/dmd.116.074104
This article has not been copyedited and formatted. The final version may differ from this version.

NIM and its main metabolites on bile acid transporters using sandwich-cultured human and rat hepatocytes to reveal a possible mechanism for NIM-induced cholestasis.

A previous study (Warrington et al., 1993) reported that NIM 800 mg daily was tolerated in healthy men with only minor renal toxicity. When corrected for interspecies differences with the dose scaling factor of 6.167 (Singh et al., 2012), the dose of 800 mg daily for humans corresponds to 82.2 mg/kg/day for rats. Our pilot studies showed that 200 mg/kg/day of NIM was a lethal dose to rats, while 50 mg/kg/day dose did not show significant liver toxicity. Taken together, 100 mg/kg/day dose was selected to investigate the cholestatic effect of NIM in rats.

The rats pretreated with 100 mg/kg/day NIM for 5 days via oral administration was associated with a significant increase in plasma levels of AST, ALT, ALP, and TBA, which are markers of cholestasis and hepatotoxicity (Fattinger et al., 2001; Funk et al., 2001a; Kostrubsky et al., 2003; Li et al., 2015). Meanwhile, the biliary secretion of bile acids significantly decreased in the NIM-treated rats. Theoretically, the decreased biliary secretion of bile acids could lead to reduced bile flow (Yoshikado et al., 2011; Li et al., 2016). However, in our study, there was no significant difference in the bile flow rate between the NIM-treated and the non-treated rats. We speculated that hepatic glutathione levels which markedly increased in the NIM-treated rats (data not shown) possibly caused an increase of bile flow and eventually offset the decreased bile flow dependent on bile acids. It has been reported that secretion of glutathione is a driving force for the generation of

Downloaded from dmd.aspetjournals.org at ASPET Journals on April 18, 2024

DMD Fast Forward. Published on February 15, 2017 as DOI: 10.1124/dmd.116.074104
This article has not been copyedited and formatted. The final version may differ from this version.

canalicular bile flow besides bile acids (Ballatori and Truong, 1992; Zsembery et al., 2000).

Inhibition of hepatobiliary transporters responsible for bile acid uptake and efflux by the parent drug and/or its metabolites is one possible mechanism leading to cholestasis (Funk et al., 2001b; McRae et al., 2006; Li et al., 2015; Slizgi et al., 2016). NIM underwent extensive metabolism in rats, similar to the metabolic fate in humans. M1 was the major metabolite in rat plasma, whereas M1, M2, and M4 were the major metabolites in rat liver. We then evaluated the effects of NIM and its metabolites (M1, M2, and M4) on bile acid transporters.

First, we explored the effects of NIM, M1, M2, and M4 on the transport of d_8-TCA, a probe substrate for NTCP, OATPs, and BSEP (Lepist et al., 2014; Li et al., 2015; Slizgi et al., 2016), in sandwich-cultured rat hepatocytes. Both NIM and M1 reduced the $Cl_{biliary}$ and BEI values of d_8-TCA in a concentration-dependent manner. Reduction in BEI suggested that NIM and M1 inhibited the BSEP-mediated excretion of d_8-TCA into the canalicular lumen. $Cl_{biliary}$ is an indicator of the overall effects of test compounds on bile acid excretion. Reduction in $Cl_{biliary}$ under NIM and M1 treatments possibly resulted from the inhibition of basolateral uptake transporters and/or canalicular efflux transporters. $Cl_{biliary}$ of d_8-TCA was inhibited to a larger extent than BEI under NIM and M1 treatments, demonstrating that NIM and M1 exerted a greater inhibitory effect on the uptake than on the efflux of d_8-TCA. Troglitazone and bosentan, which cause cholestasis in clinics, displayed similar effects on the hepatobiliary disposition of d_8-TCA as observed for NIM and M1

Downloaded from dmd.aspetjournals.org at ASPET Journals on April 18, 2024

DMD Fast Forward. Published on February 15, 2017 as DOI: 10.1124/dmd.116.074104
This article has not been copyedited and formatted. The final version may differ from this version.

(Ansede et al., 2010). The inhibitory effects of NIM and M1 on rat NTCP and OATPs were further evaluated using suspended rat hepatocytes. NIM and M1 exerted greater inhibitory effects on NTCP than on OATPs, as indicated by lower IC_{50} values of these compounds toward NTCP than toward OATPs.

BEI of d_8-TCA barely changed under M2 and M4 treatments, suggesting that these compounds did not interfere with BSEP activity. Moreover, $Cl_{biliary}$ of d_8-TCA slightly decreased under M2 and M4 treatments, indicating that d_8-TCA uptake was weakly inhibited. However, given the extremely low concentrations of M2 and M4 in rat plasma, their inhibitory effects on the uptake transporters were negligible.

In addition to NTCP, OATPs and BSEP, MRPs are important transporters mediating the transport of bile acids, especially the sulfated bile acids (Akita et al., 2001; Morgan et al., 2013; Rodrigues et al., 2014). We explored the inhibitory effects of NIM and its metabolites on rat MRP2/3 by using CDF as probe substrate. NIM and M1 (200 μM each) significantly reduced the fluorescent signal of CDF in bile canaliculi, similar to the effect of MK-571. Additionally, concentration-dependent reduction in BEI of CDF was observed under NIM and M1 treatments. Both results suggested that NIM and M1 inhibited MRP2-mediated CDF excretion. Furthermore, NIM and M1 decreased the basolateral efflux of CDF (Fig. 7), consistent with the increase in cellular plus biliary accumulation of CDF (Fig. 6), indicating that the basolateral efflux transporter MRP3 was also inhibited by NIM and M1. Dual inhibition of two different excretory pathways, namely, MRP2- and MRP3-mediated effluxes, may lead to marked increase of some bile acids. By contrast, M2 and M4 did

Downloaded from dmd.aspetjournals.org at ASPET Journals on April 18, 2024

DMD Fast Forward. Published on February 15, 2017 as DOI: 10.1124/dmd.116.074104
This article has not been copyedited and formatted. The final version may differ from this version.

not or slightly reduced the fluorescent signal of CDF in bile canaliculi, suggesting that these metabolites did not inhibit or they only marginally inhibited MRP2.

In addition to CDF, d_8-TCA can be used as probe substrate to evaluate the function of MRP3 (Guo et al., 2014). We attempted to use d_8-TCA to characterize the function of MRP3. Unexpectedly, the content of d_8-TCA in the efflux medium was not reduced but rather slightly increased in the presence of NIM or M1 (data not shown), possibly because that the NTCP-mediated reuptake of TCA was inhibited. Compared with d_8-TCA, CDF was a substrate for OATPs rather than for NTCP (Zamek-Gliszczynski et al., 2003). NIM and M1 exerted considerably weaker inhibitory effects on OATPs than NTCP, thus CDF content in the efflux medium was mainly dependent on the effects of NIM and M1 on MRP3.

The effects of NIM and M1 on human bile acid transporters were also investigated using sandwich-cultured human hepatocytes. Similar to the results from rat hepatocytes studies, the $Cl_{biliary}$ of d_8-TCA was inhibited to a larger extent than BEI under NIM and M1 treatments, indicating that NIM and M1 exerted a greater inhibitory effect on the uptake transporters than on the efflux transporter of d_8-TCA. Besides, the inhibitory effects of NIM and M1 on MRP2 were confirmed by the reduced fluorescent signal of CDF in bile canaliculi.

Overall, both NIM and M1 demonstrated inhibitory effects on the uptake transporters NTCP and OATPs and on the efflux transporters BSEP and MRP2. However, the reduced metabolites of NIM (M2 and M4) did not inhibit or they only marginally inhibited these bile acid transporters. The current result suggests that

Downloaded from dmd.aspetjournals.org at ASPET Journals on April 18, 2024

DMD Fast Forward. Published on February 15, 2017 as DOI: 10.1124/dmd.116.074104
This article has not been copyedited and formatted. The final version may differ from this version.

inhibition of bile acid transporters by NIM and M1 may negatively impact bile acid homeostasis, which may explain, at least in part, the mechanism of NIM-induced cholestasis.

Downloaded from dmd.aspetjournals.org at ASPET Journals on April 18, 2024

DMD Fast Forward. Published on February 15, 2017 as DOI: 10.1124/dmd.116.074104
This article has not been copyedited and formatted. The final version may differ from this version.

Acknowledgments

We thank Dr. Xiuli Li for helpful discussions. We also thank Hua Cao and Ziqing Zuo for their kind help in synthesizing the metabolites of NIM.

Authorship Contributions

Participated in research design: Zhou, Pang, Chen.

Conducted experiments: Zhou, Pang, Jiang.

Contributed new reagents or analytic tools: Zhou, Pang, Chen.

Performed data analysis: Zhou, Pang, Chen.

Contributed to the writing of the manuscript: Zhou, Chen, Zhong.

Downloaded from dmd.aspetjournals.org at ASPET Journals on April 18, 2024

DMD Fast Forward. Published on February 15, 2017 as DOI: 10.1124/dmd.116.074104
This article has not been copyedited and formatted. The final version may differ from this version.

References

Akita H, Suzuki H, Ito K, Kinoshita S, Sato N, Takikawa H, and Sugiyama Y (2001) Characterization of bile acid transport mediated by multidrug resistance associated protein 2 and bile salt export pump. *Biochim Biophys Acta* **1511:**7-16.

Alrefai WA and Gill RK (2007) Bile acid transporters: structure, function, regulation and pathophysiological implications. *Pharm Res* **24:**1803-1823.

Ansede JH, Smith WR, Perry CH, Claire RLS, and Brouwer KR (2010) An in vitro assay to assess transporter-based cholestatic hepatotoxicity using sandwich-cultured rat hepatocytes. *Drug Metab Dispos* **38:**276-280.

Ballatori N and Truong AT (1992) Glutathione as a primary osmotic driving force in hepatic bile formation. *Am J Physiol* **263:**G617-G624.

Carini M, Aldini G, Stefani R, Marinello C, and Facino RM (1998) Mass spectrometric characterization and HPLC determination of the main urinary metabolites of nimesulide in man. *J Pharm Biomed Anal* **18:**201-211.

Chandra P, Zhang P, and Brouwer KL (2005) Short-term regulation of multidrug resistance-associated protein 3 in rat and human hepatocytes. *Am J Physiol Gastrointest Liver Physiol* **288:**G1252-G1258.

Dawson S, Stahl S, Paul N, Barber J, and Kenna JG (2012) In vitro inhibition of the bile salt export pump correlates with risk of cholestatic drug-induced liver injury in humans. *Drug Metab Dispos* **40:**130-138.

Fattinger K, Funk C, Pantze M, Weber C, Reichen J, Stieger B, and Meier PJ (2001)

Downloaded from dmd.aspetjournals.org at ASPET Journals on April 18, 2024

DMD Fast Forward. Published on February 15, 2017 as DOI: 10.1124/dmd.116.074104
This article has not been copyedited and formatted. The final version may differ from this version.

The endothelin antagonist bosentan inhibits the canalicular bile salt export pump: a potential mechanism for hepatic adverse reactions. *Clin Pharmacol Ther* **69:**223-231.

Funk C, Pantze M, Jehle L, Ponelle C, Scheuermann G, Lazendic M, and Gasser R (2001a) Troglitazone-induced intrahepatic cholestasis by an interference with the hepatobiliary export of bile acids in male and female rats. Correlation with the gender difference in troglitazone sulfate formation and the inhibition of the canalicular bile salt export pump (Bsep) by troglitazone and troglitazone sulfate. *Toxicology* **167:**83-98.

Funk C, Ponelle C, Scheuermann G, and Pantze M (2001b) Cholestatic potential of troglitazone as a possible factor contributing to troglitazone-induced hepatotoxicity: in vivo and in vitro interaction at the canalicular bile salt export pump (Bsep) in the rat. *Mol Pharmacol* **59:**627-635.

Gandini R, Montalto C, Castoldi D, Monzani V, Nava ML, Scaricabarozzi I, Vargiu G, and Bartosek I (1991) First dose and steady state pharmacokinetics of nimesulide and its 4-hydroxy metabolite in healthy volunteers. *Farmaco* **46:**1071-1079.

Guo C, He L, Yao D, A J, Cao B, Ren J, Wang G, and Pan G (2014) Alpha-naphthylisothiocyanate modulates hepatobiliary transporters in sandwich-cultured rat hepatocytes. *Toxicol Lett* **224:**93-100.

Halilbasic E, Claudel T, and Trauner M (2013) Bile acid transporters and regulatory nuclear receptors in the liver and beyond. *J Hepatol* **58:**155-168.

Downloaded from dmd.aspetjournals.org at ASPET Journals on April 18, 2024

DMD Fast Forward. Published on February 15, 2017 as DOI: 10.1124/dmd.116.074104
This article has not been copyedited and formatted. The final version may differ from this version.

Küçükgüzel SG, Küçükgüzel I, Oral B, Sezen S, and S. R (2005) Detection of nimesulide metabolites in rat plasma and hepatic subcellular fractions by HPLC-UV/DAD and LC-MS/MS studies. *Eur J Drug Metab Pharmacokinet* **30:**127-134.

Kostrubsky VE, Strom SC, Hanson J, Urda E, Rose K, Burliegh J, Zocharski P, Cai H, Sinclair JF, and Sahi J (2003) Evaluation of hepatotoxic potential of drugs by inhibition of bile-acid transport in cultured primary human hepatocytes and intact rats. *Toxicol Sci* **76:**220-228.

Lepist EI, Gillies H, Smith W, Hao J, Hubert C, St Claire RL, 3rd, Brouwer KR, and Ray AS (2014) Evaluation of the endothelin receptor antagonists ambrisentan, bosentan, macitentan, and sitaxsentan as hepatobiliary transporter inhibitors and substrates in sandwich-cultured human hepatocytes. *PLoS One* **9:**e87548.

Li F, Chordia MD, Huang T, and Macdonald TL (2008) In vitro nimesulide studies toward understanding idiosyncratic hepatotoxicity: diiminoquinone formation and conjugation. *Chem Res Toxicol* **22:**72-80.

Li X, Liu R, Luo L, Yu L, Chen X, Sun L, Wang T, Hylemon PB, Zhou H, Jiang Z, and Zhang L (2016) Role of AMP-activated protein kinase alpha1 in 17alpha-ethinylestradiol-induced cholestasis in rats. *Arch Toxicol* doi:10.1007/s00204-016-1697-8.

Li X, Zhong K, Guo Z, Zhong D, and Chen X (2015) Fasiglifam (TAK-875) inhibits hepatobiliary transporters: a possible factor contributing to fasiglifam-induced liver injury. *Drug Metab Dispos* **43:**1751-1759.

Downloaded from dmd.aspetjournals.org at ASPET Journals on April 18, 2024

DMD Fast Forward. Published on February 15, 2017 as DOI: 10.1124/dmd.116.074104
This article has not been copyedited and formatted. The final version may differ from this version.

Liu X, LeCluyse EL, Brouwer KR, Gan LS, Lemasters JJ, Stieger B, Meier PJ, and Brouwer KL (1999) Biliary excretion in primary rat hepatocytes cultured in a collagen-sandwich configuration. *Am J Physiol* **277:**G12–G21.

Macpherson D, Best SA, Gedik L, Hewson AT, Rainsford KD, and Parisi S (2013) The Biotransformation and Pharmacokinetics of 14C-Nimesulide in Humans Following a Single Dose Oral Administration. *J Drug Metab Toxicol* **4:**140.

Marion TL, Perry CH, Claire RLS, Yue W, and Brouwer KLR (2011) Differential disposition of chenodeoxycholic acid versus taurocholic acid in response to acute troglitazone exposure in rat hepatocytes. *Toxicol Sci* **120:**371-380.

McRae MP, Lowe CM, Tian X, Bourdet DL, Ho RH, Leake BF, Kim RB, Brouwer KL, and Kashuba AD (2006) Ritonavir, saquinavir, and efavirenz, but not nevirapine, inhibit bile acid transport in human and rat hepatocytes. *J Pharmacol Exp Ther* **318:**1068-1075.

Mingatto FE, Rodrigues T, Pigoso AA, Uyemura SA, Curti C, and Santos AC (2002) The critical role of mitochondrial energetic impairment in the toxicity of nimesulide to hepatocytes. *J Pharmacol Exp Ther* **303:**601-607.

Morgan RE, van Staden CJ, Chen Y, Kalyanaraman N, Kalanzi J, Dunn RT, Afshari CA, and Hamadeh HK (2013) A multifactorial approach to hepatobiliary transporter assessment enables improved therapeutic compound development. *Toxicol Sci* **136:**216-241.

Rodrigues AD, Lai Y, Cvijic ME, Elkin LL, Zvyaga T, and Soars MG (2014) Drug-induced perturbations of the bile acid pool, cholestasis, and

Downloaded from dmd.aspetjournals.org at ASPET Journals on April 18, 2024

DMD Fast Forward. Published on February 15, 2017 as DOI: 10.1124/dmd.116.074104
This article has not been copyedited and formatted. The final version may differ from this version.

hepatotoxicity: mechanistic considerations beyond the direct inhibition of the bile salt export pump. *Drug Metab Dispos* **42:**566-574.

Romero-Gomez M, Nevado Santos M, Otero Fernandez MA, Fovelo MJ, Suarez-Garcia E, and Castro Fernandez M (1999) Acute cholestatic hepatitis induced by nimesulide. *Liver* **19:**164-165.

Saab L, Peluso J, Muller CD, and Ubeaud-Sequier G (2013) Implication of hepatic transporters (MDR1 and MRP2) in inflammation-associated idiosyncratic drug-induced hepatotoxicity investigated by microvolume cytometry. *Cytometry A* **83:**403-408.

Singh BK, Tripathi M, Chaudhari BP, Pandey PK, and Kakkar P (2012) Natural terpenes prevent mitochondrial dysfunction, oxidative stress and release of apoptotic proteins during nimesulide-hepatotoxicity in rats. *PLoS One* **7:**e34200.

Slizgi JR, Lu Y, Brouwer KR, St Claire RL, Freeman KM, Pan M, Brock WJ, and Brouwer KL (2016) Inhibition of Human Hepatic Bile Acid Transporters by Tolvaptan and Metabolites: Contributing Factors to Drug-Induced Liver Injury? *Toxicol Sci* **149:**237-250.

Stadlmann S, Zoller H, Vogel W, and Offner FA (2002) COX-2 inhibitor (nimesulide) induced acute liver failure. *Virchows Arch* **440:**553-555.

Stieger B, Fattinger K, Madon J, Kullak-Ublick GA, and Meier PJ (2000) Drug-and estrogen-induced cholestasis through inhibition of the hepatocellular bile salt export pump (Bsep) of rat liver. *Gastroenterology* **118:**422-430.

Downloaded from dmd.aspetjournals.org at ASPET Journals on April 18, 2024

DMD Fast Forward. Published on February 15, 2017 as DOI: 10.1124/dmd.116.074104
This article has not been copyedited and formatted. The final version may differ from this version.

Warrington SJ, Ravic M, and Dawnay A (1993) Renal and general tolerability of repeated doses of nimesulide in normal subjects. *Drugs* **46 Suppl 1:**263-269.

Yoshikado T, Takada T, Yamamoto T, Yamaji H, Ito K, Santa T, Yokota H, Yatomi Y, Yoshida H, Goto J, Tsuji S, and Suzuki H (2011) Itraconazole-induced cholestasis: involvement of the inhibition of bile canalicular phospholipid translocator MDR3/ABCB4. *Mol Pharmacol* **79:**241-250.

Zamek-Gliszczynski MJ, Xiong H, Patel NJ, Turncliff RZ, Pollack GM, and Brouwer KL (2003) Pharmacokinetics of 5 (and 6)-carboxy-2',7'-dichlorofluorescein and its diacetate promoiety in the liver. *J Pharmacol Exp Ther* **304:**801-809.

Zhang P, Tian X, Chandra P, and Brouwer KLR (2005) Role of glycosylation in trafficking of Mrp2 in sandwich-cultured rat hepatocytes. *Mol Pharmacol* **67:**1334-1341.

Zhou L, Pang X, Xie C, Zhong D, and Chen X (2015) Chemical and Enzymatic Transformations of Nimesulide to GSH Conjugates through Reductive and Oxidative Mechanisms. *Chem Res Toxicol* **28:**2267-2277.

Zsembery A, Thalhammer T, and Graf J (2000) Bile Formation: a Concerted Action of Membrane Transporters in Hepatocytes and Cholangiocytes. *News Physiol Sci* **15:**6-11.

Downloaded from dmd.aspetjournals.org at ASPET Journals on April 18, 2024

DMD Fast Forward. Published on February 15, 2017 as DOI: 10.1124/dmd.116.074104
This article has not been copyedited and formatted. The final version may differ from this version.

Footnotes

Conflicts of Interest: The authors declare no conflicts of interest.

Financial Support: This work was supported by the National Natural Science Foundation of China [81573500 and 81503153].

Downloaded from dmd.aspetjournals.org at ASPET Journals on April 18, 2024

DMD Fast Forward. Published on February 15, 2017 as DOI: 10.1124/dmd.116.074104
This article has not been copyedited and formatted. The final version may differ from this version.

Figure Legends

Fig. 1. Simplified metabolic pathways of NIM.

Fig. 2. Effects of NIM on (A) activities of plasma AST, ALT, and ALP, (B) plasma TBA level, (C) biliary secretion of bile acids, and (D) bile flow rate in Wistar rats. Data are reported as mean ± SD (n = 4 or 6). $^{*}P < 0.05$ and $^{**}P < 0.01$ vs. the control group.

Fig. 3. Effects of NIM and its metabolites (M1, M2, and M4) on the accumulation, BEI, and $Cl_{biliary}$ of d_8-TCA (1 μM) in sandwich-cultured rat hepatocytes. CyA (10 μM) was used as the positive inhibitor. (A) d_8-TCA accumulation was measured in standard buffer (cells plus bile, solid bars) or Ca^{2+}-free buffer (cells only, open bars) for 10 min. (B) BEI and $Cl_{biliary}$ of d_8-TCA in the presence of potential inhibitors are expressed as percentages of control. Data were compiled from at least three separate rat liver preparations and are reported as mean ± SD. $^{*}P < 0.05$, $^{**}P < 0.01$, and $^{***}P < 0.001$ vs. the control group.

Fig. 4. (A) Effects of NIM and its metabolites (M1, M2, and M4) on d_8-TCA uptake by rat hepatocytes incubated in Na^{+}-containing buffer (open bar) or in Na^{+}-free buffer (solid bar). Inhibitory effects of (B) NIM and (C) M1 on NTCP- and OATP-mediated d_8-TCA uptake by rat hepatocytes. Uptake was measured after 2 min of incubation with 1 μM d_8-TCA. CyA (10 μM) was used as the positive control. Data were compiled from at least three separate rat liver preparations and are presented as mean ± SD. $^{**}P < 0.01$ and $^{***}P < 0.001$ vs. the control group.

Fig. 5. CDF disposition in sandwich-cultured rat hepatocytes as measured by

Downloaded from dmd.aspetjournals.org at ASPET Journals on April 18, 2024

DMD Fast Forward. Published on February 15, 2017 as DOI: 10.1124/dmd.116.074104
This article has not been copyedited and formatted. The final version may differ from this version.

fluorescence microscopy after 10 min of incubation in standard buffer. Cells treated with (A) vehicle only, (B) 200 μM NIM, (C) 200 μM M1, (D) 400 μM M2, (E) 200 μM M4, and (F) 20 μM MK-571 (as the positive inhibitor). White arrows indicate the representative tubular structures of the bile canalicular network.

Fig. 6. Effects of NIM and M1 on the accumulation and BEI of CDF in sandwich-cultured rat hepatocytes. CDF accumulation in sandwich-cultured rat hepatocytes was measured in standard buffer (cells plus bile, solid bars) or in Ca^{2+}-free buffer (cells only, open bars) for 10 min. Data are expressed as percentages of control (accumulation in the standard buffer), mean ± SD of at least three independent experiments. $^{*}P < 0.05$, $^{**}P < 0.01$, and $^{***}P < 0.001$ vs. the control group.

Fig. 7. Effects of NIM and M1 on the basolateral efflux of CDF in sandwich-cultured rat hepatocytes. MK-571 (20 μM) was used as the positive inhibitor. Data were compiled from at least three separate rat liver preparations and are expressed as mean ± SD. $^{*}P < 0.05$, $^{**}P < 0.01$, and $^{***}P < 0.001$ vs. the control group.

Fig. 8. Effects of NIM and M1 on the accumulation, BEI, and $Cl_{biliary}$ of d_8-TCA (1 μM) in sandwich-cultured human hepatocytes. CyA (10 μM) was used as the positive inhibitor. d_8-TCA accumulation was measured in standard buffer (cells plus bile, solid bars) or Ca^{2+}-free buffer (cells only, open bars) for 10 min. Data are reported as mean ± SD of one experiment in triplicate. The experiment was repeated and the same trend was observed. $^{***}P < 0.001$ vs. the control group.

Fig. 9. CDF disposition in sandwich-cultured human hepatocytes as measured by

Downloaded from dmd.aspetjournals.org at ASPET Journals on April 18, 2024

DMD Fast Forward. Published on February 15, 2017 as DOI: 10.1124/dmd.116.074104
This article has not been copyedited and formatted. The final version may differ from this version.

fluorescence microscopy after 10 min of incubation in standard buffer. Cells treated with (A) vehicle only, (B) 200 μM NIM, (C) 200 μM M1, and (D) 20 μM MK-571 (as the positive inhibitor). White arrows indicate the representative tubular structures of the bile canalicular network.

Downloaded from dmd.aspetjournals.org at ASPET Journals on April 18, 2024

DMD Fast Forward. Published on February 15, 2017 as DOI: 10.1124/dmd.116.074104
This article has not been copyedited and formatted. The final version may differ from this version.

TABLE 1 Plasma bile acid levels in rats orally administered with 100 mg/kg/day NIM or with 0.5% CMC-Na for 5 days. Blood samples were collected at 24 h after the last dose. Data are reported as mean ± SD (n = 6)

No.	Bile acid (ng/mL)	Control	NIM	Fold
1	CA[a]	2530 ± 1050	7233 ± 2845	2.86
2	DCA[a]	290 ± 107	779 ± 424	2.68
3	CDCA[a]	928 ± 221	3593 ± 1767	3.87
4	UDCA[a]	1143 ± 413	3433 ± 2082	3.00
5	LCA	47 ± 17	76 ± 48	1.62
6	GCA	376 ± 84	388 ± 183	1.03
7	GDCA	166 ± 25	148 ± 37	0.89
8	GCDCA	140 ± 54	195 ± 44	1.39
9	GUDCA	113 ± 23	157 ± 45	1.39
10	TCA	55 ± 3	41 ± 12	0.74
11	TCDCA	59 ± 11	46 ± 15	0.77

[a]Indicates > 2-fold increase compared with the control.

Downloaded from dmd.aspetjournals.org at ASPET Journals on April 18, 2024

DMD Fast Forward. Published on February 15, 2017 as DOI: 10.1124/dmd.116.074104
This article has not been copyedited and formatted. The final version may differ from this version.

TABLE 2 Liver bile acid levels in rats orally administered with 100 mg/kg/day NIM or with 0.5% CMC-Na for 5 days. Liver samples were collected at 24 h after the last dose. Data are reported as mean ± SD (n = 6)

No.	Bile acid (ng/mL)	Control	NIM	Fold
1	CA[a]	69 ± 6	199 ± 43	2.88
2	DCA	NA	NA	
3	CDCA[a]	67 ± 16	137 ± 43	2.04
4	UDCA	58 ± 23	93 ± 40	1.60
5	LCA	NA	NA	
6	GCA	611 ± 384	551 ± 537	0.90
7	GDCA	57 ± 28	103 ± 98	1.81
8	GCDCA[a]	104 ± 38	252 ± 157	2.42
9	GUDCA	105 ± 49	164 ± 91	1.56
10	TCA	4045 ± 990	6468 ± 1801	1.60
11	TCDCA	4620 ± 592	5055 ± 2192	1.09

[a]Indicates > 2-fold increase compared with the control. NA: not assayed.

Downloaded from dmd.aspetjournals.org at ASPET Journals on April 18, 2024

DMD Fast Forward. Published on February 15, 2017 as DOI: 10.1124/dmd.116.074104
This article has not been copyedited and formatted. The final version may differ from this version.

TABLE 3 Concentrations of NIM and its metabolites (M1, M2, and M4) in rat plasma and liver tissue at 24 h after the last dose of NIM. The rats were orally administered with 100 mg/kg/day NIM for 5 days. Data are reported as mean ± SD (*n* = 6)

Metabolites	Concentration (μM)	
	Plasma	Liver tissue
NIM	45.4 ± 19.4	17.3 ± 10.1
M1	21.0 ± 1.9	23.6 ± 7.6
M2	0.037 ± 0.020	1.80 ± 0.62
M4	0.180 ± 0.113	13.4 ± 8.9

Downloaded from dmd.aspetjournals.org at ASPET Journals on April 18, 2024

DMD Fast Forward. Published on February 15, 2017 as DOI: 10.1124/dmd.116.074104
This article has not been copyedited and formatted. The final version may differ from this version.

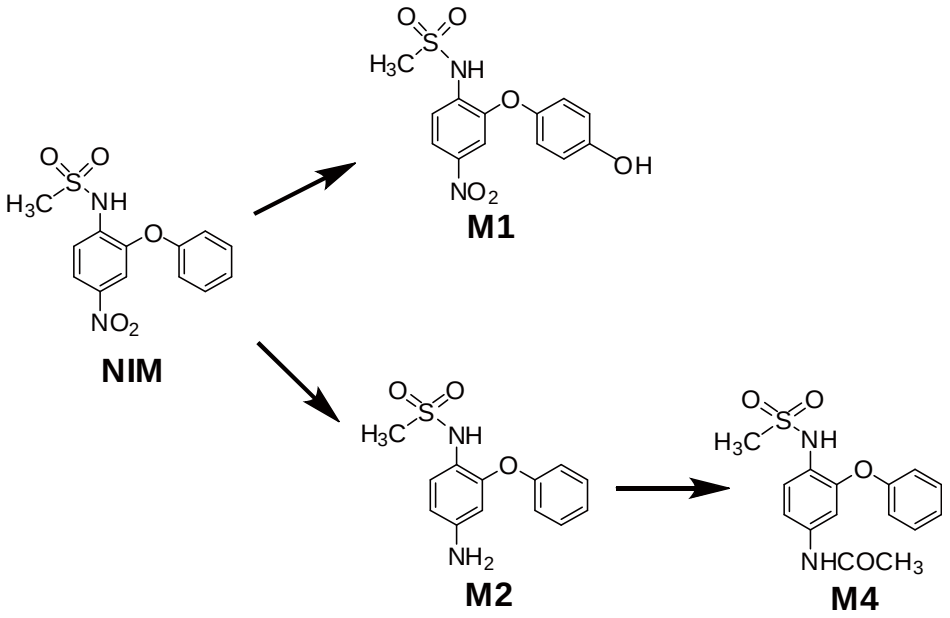

Figure 1

Downloaded from dmd.aspetjournals.org at ASPET Journals on April 18, 2024

DMD Fast Forward. Published on February 15, 2017 as DOI: 10.1124/dmd.116.074104
This article has not been copyedited and formatted. The final version may differ from this version.

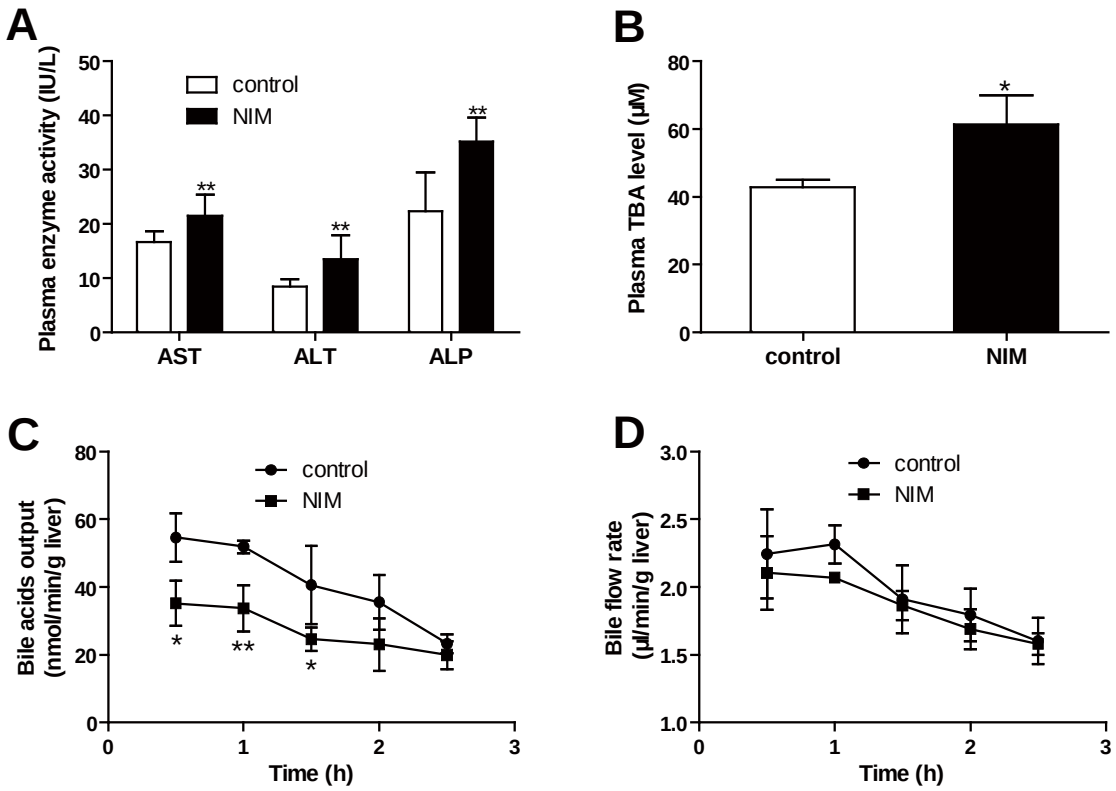

Figure 2

Downloaded from dmd.aspetjournals.org at ASPET Journals on April 18, 2024

DMD Fast Forward. Published on February 15, 2017 as DOI: 10.1124/dmd.116.074104
This article has not been copyedited and formatted. The final version may differ from this version.

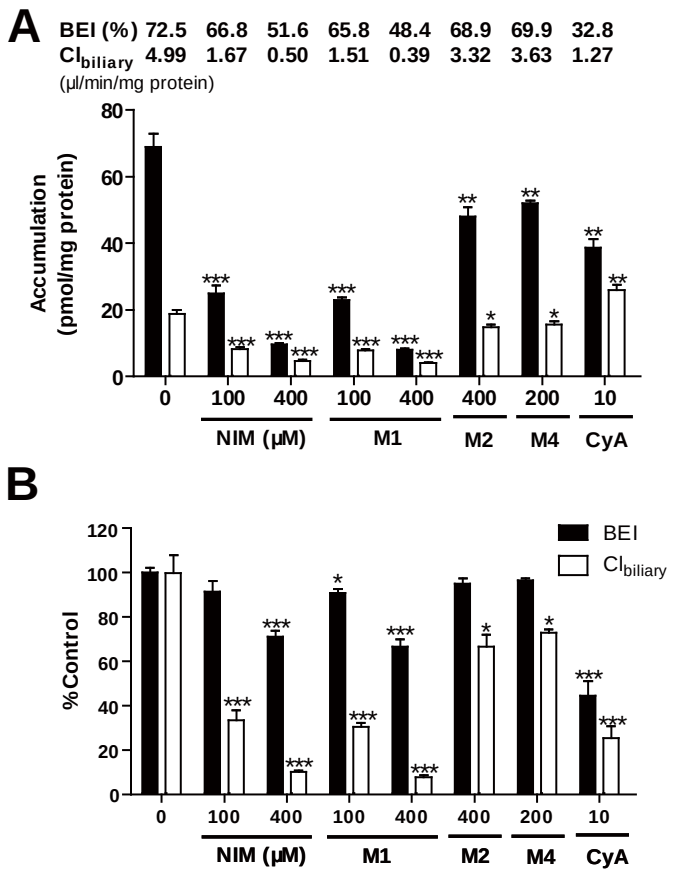

Figure 3

Downloaded from dmd.aspetjournals.org at ASPET Journals on April 18, 2024

DMD Fast Forward. Published on February 15, 2017 as DOI: 10.1124/dmd.116.074104
This article has not been copyedited and formatted. The final version may differ from this version.

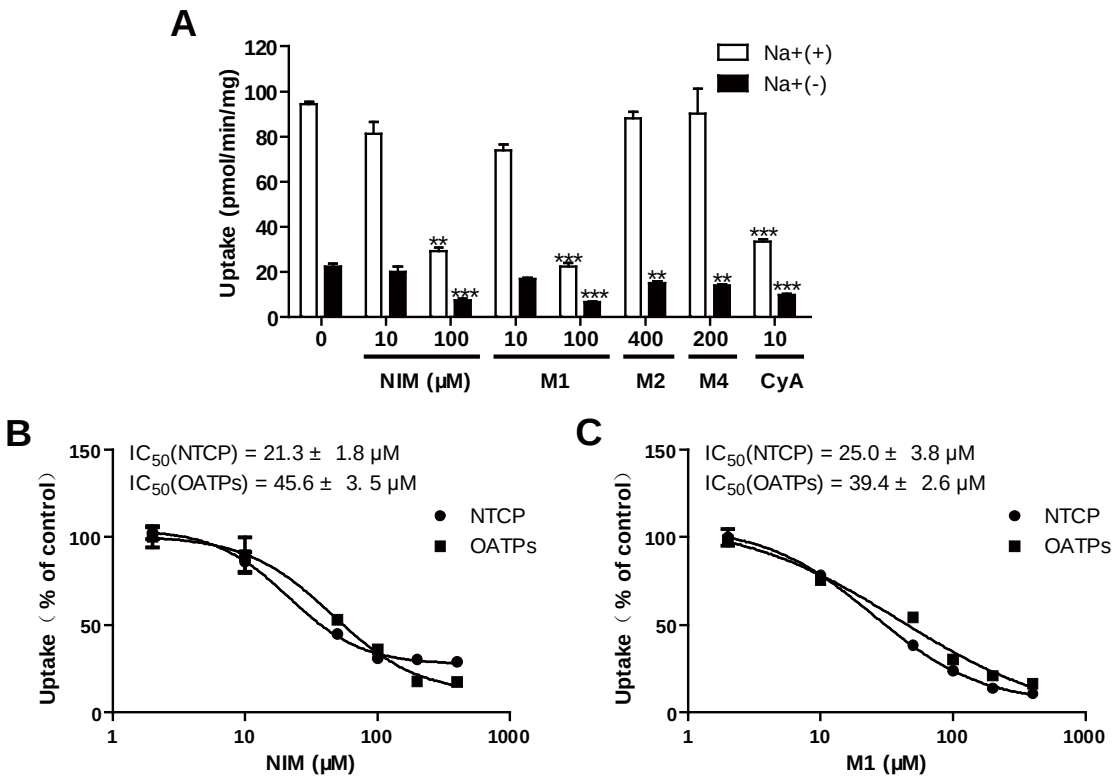

Figure 4

Downloaded from dmd.aspetjournals.org at ASPET Journals on April 18, 2024

DMD Fast Forward. Published on February 15, 2017 as DOI: 10.1124/dmd.116.074104
This article has not been copyedited and formatted. The final version may differ from this version.

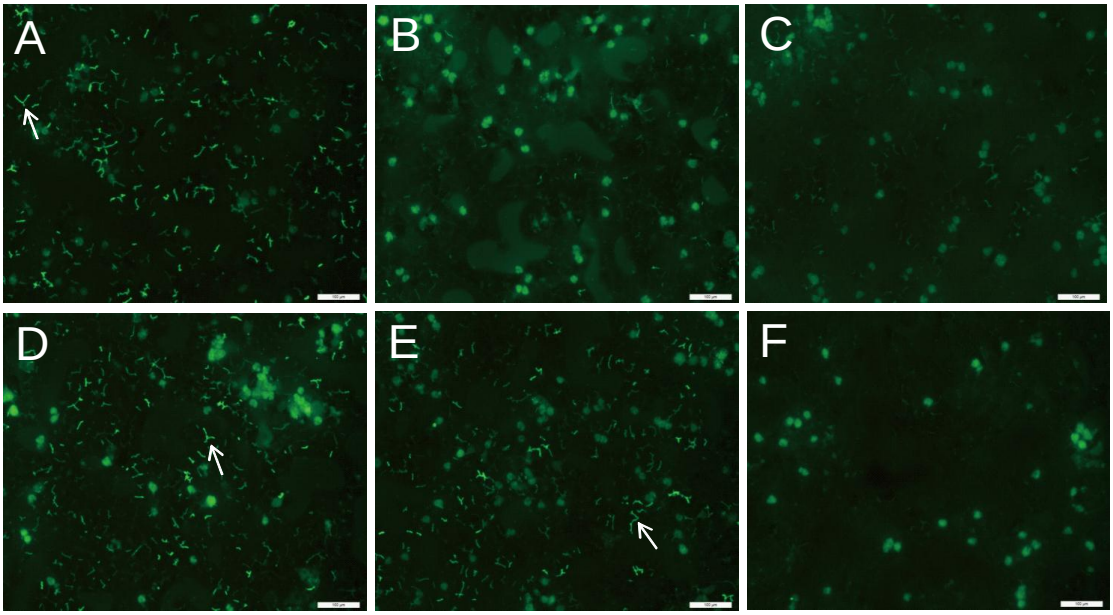

Figure 5

Downloaded from dmd.aspetjournals.org at ASPET Journals on April 18, 2024

DMD Fast Forward. Published on February 15, 2017 as DOI: 10.1124/dmd.116.074104
This article has not been copyedited and formatted. The final version may differ from this version.

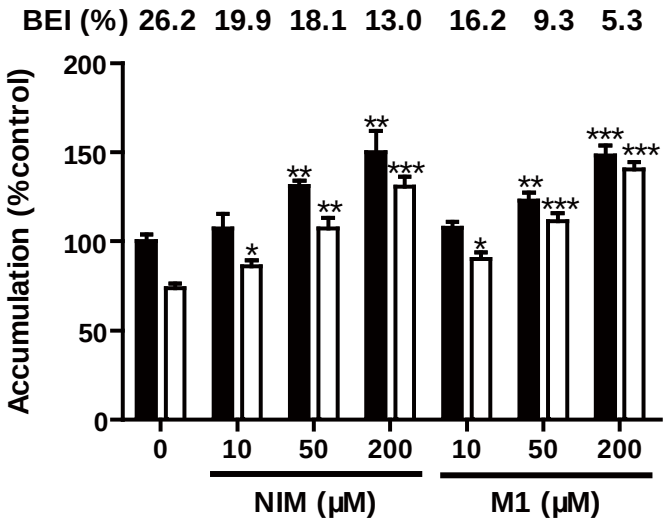

Figure 6

Downloaded from dmd.aspetjournals.org at ASPET Journals on April 18, 2024

DMD Fast Forward. Published on February 15, 2017 as DOI: 10.1124/dmd.116.074104
This article has not been copyedited and formatted. The final version may differ from this version.

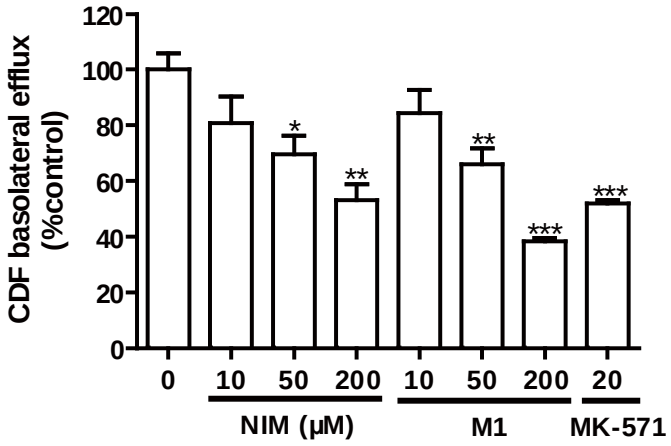

Figure 7

Downloaded from dmd.aspetjournals.org at ASPET Journals on April 18, 2024

DMD Fast Forward. Published on February 15, 2017 as DOI: 10.1124/dmd.116.074104
This article has not been copyedited and formatted. The final version may differ from this version.

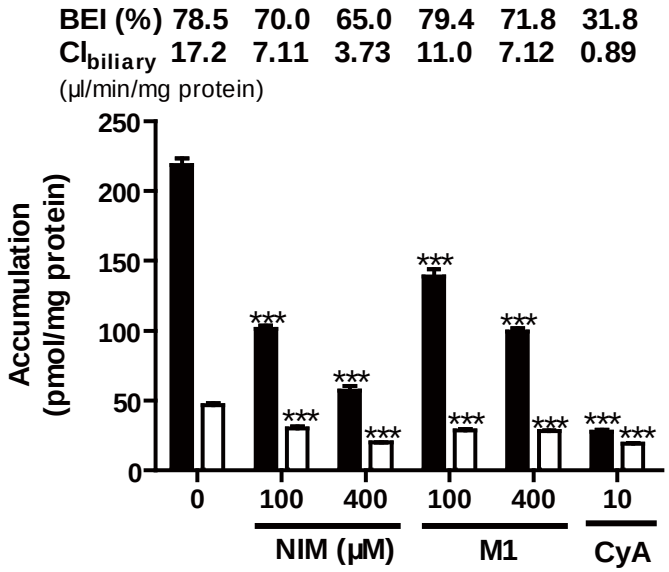

Figure 8

Downloaded from dmd.aspetjournals.org at ASPET Journals on April 18, 2024

DMD Fast Forward. Published on February 15, 2017 as DOI: 10.1124/dmd.116.074104
This article has not been copyedited and formatted. The final version may differ from this version.

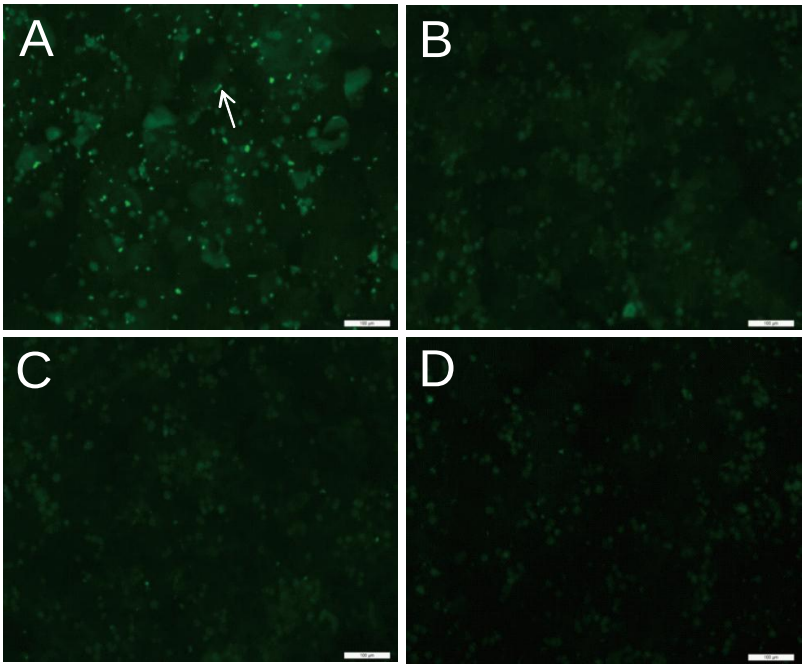

Figure 9

Downloaded from dmd.aspetjournals.org at ASPET Journals on April 18, 2024